Supporting Information for

$LiGa_5O_8$:Cr-based theranostic nanoparticles for imaging-guided X-ray induced photodynamic therapy of deep-seated tumors

Supplementary Experimental Section:

Synthesis of LGO:Cr nanoparticles: Stoichiometric amounts of lithium nitrate, gallium nitrate, and chromium nitrate were dissolved in methanol. The solution was magnetically stirred for 5 hours. During the process, a chelating agent, acetylacetone, and polystyrene spheres were added into the solution. Aqueous ammonium solution (28 vol.%) was added to the solution to stabilize the resulting complexes and adjust its pH. When a homogeneous sol was formed, the solution was heated to 80-100 °C for several hours to form a dry gel. The dry gel was then calcinated in a muffle furnace at 1000-1100°C for 3-5 h to form LGO:Cr powder. To render LGO:Cr powder amenable to bio-related applications, we wet ground LGO:Cr powders into nanoparticles. After filtration and centrifugation, LGO:Cr nanoparticles with a diameter of about 100 nm were obtained.

Surface modification of LGO:Cr: The size selection of LGO:Cr nanoparticles and surface modification with tetraethyl orthosilicate (TEOS) and (3-Aminopropyl)triethoxysilane (APTES) were conducted based on our published protocol.[1, 2] Briefly, 10 mg of LGO:Cr nanoparticles were dispersed in a mixture of 40 mL of H_2O, 5 mg cetrimonium bromide (CTAB), and 1 mL of 28-30% ammonia. After stirring for 30 min, 10 µL of TEOS and 5 µL of APTES were added, and the mixture was magnetically stirred at 70 ˚C for 3 hrs. CTAB was removed by incubating the particles in a NH_4Cl/EtOH solution. This results in the formation of amine-presenting mesoporous silica coated LGO:Cr (LGO:Cr@$mSiO_2$).
For PEGylation, 5 mg of NHS-PEG-COOH (m.w.=5000) was incubated with 5 mg of LGO:Cr@$mSiO_2$ nanoparticles in PBS (pH 7.4) for 30 min. After that, the particles were centrifuged and washed with PBS (pH 7.4) for three times to obtain LGO:Cr@$mSiO_2$-PEG-COOH. To conjugate antibody (cetuximab, or CTX) onto the particle surface,

LGO:Cr@$mSiO_2$-PEG-COOH nanoparticles were first activated by mixing with 5 mg of EDC and 5 mg of NHS in PBS (pH 7.2) for 30 min. The resulting intermediate was collected by centrifugation and washed with PBS; it was then incubated with 1 mg CTX for 2 hrs. The final product, LGO:Cr@$mSiO_2$-CTX, was purified by centrifugation. CTX conjugation was confirmed by Fourier transform infrared spectroscopy on a Nicolet iS10 FT-IR Spectrometer. CTX concentration was determined by Coomassie blue assay. Briefly, LGO:Cr@$mSiO_2$-CTX nanoparticles containing 0.4 g of LGO:Cr were first suspended in 1.5 mL of PBS. 15 μL of the LGO:Cr@$mSiO_2$-CTX solution was then diluted by PBS to 150 μL. The nanoparticle solution or BSA standards were mixed with 150 μL of the Coomassie reagent (23200, Thermo Fisher) in 96-well plate. After shaking for 30 s, the absorbance at 595 nm was measured on a BioTek Synergy MX multi-mode plate reader. We then rrepared a standard curve by plotting the average blank corrected 595 nm measurement for each BSA standard vs. its concentration in μg/mL following the vendor-provided protocol. Using the standard curve, CTX concentration was determined by the equation:

$$[\mathrm{CTX}] = \left(\frac{4.8\mu g/mL \times 0.3mL}{15\mu L} \times 1.5mL\right)/0.4g = 36\mu g(\mathrm{CTX})/mg(\mathrm{LGO{:}Cr})$$

Characterization of LGO:Cr: Optical measurements were performed under ambient conditions. UV-vis absorption spectra were recorded on a Shimdzu 2450 UV-Vis spectrometer. Photoluminescence measurements were performed on a Hitachi F-7000 fluorescence spectrophotometer with an emission filter of 475 nm. X-ray excited optical luminescence (XEOL) spectrum was obtained on a Maestro imaging system coupled using an emission filter of 700 nm (X-ray was operated at 50 kV. The same irradiation condition was used throughout the study unless specified otherwise.). X-ray excited persistent luminescence intensity was analyzed on an IVIS Lumina II in vivo imaging system (PerkinElmer Inc.

Waltham, Massachusetts) in the "BLI" mode (i.e. without excitation). TEM images were acquired on an FEI Tecnai 20 transmission electron microscope. The crystal structure of LGO:Cr was analyzed by a PANalytical X'Pert PRO powder X-ray diffractometer with Cu Kα1 radiation ($\lambda = 1.5406$ Å).

XEOL Imaging of LGO:Cr@mSiO$_2$ nanoparticles: The images were acquired on an IVIS Lumina II imaging system in the BLI mode. The LGO:Cr@mSiO$_2$ nanoparticles were first stored in a dark box for 1 week to ensure complete bleaching. For XEOL imaging, LGO:Cr@mSiO$_2$ nanoparticles powder (0.2 mg) or LGO:Cr@mSiO$_2$ nanoparticles solution (1 mg/mL, 0.2 mL) were irradiated by X-ray for 1 min (0.02 Gy/min). For recharging, LGO:Cr@mSiO$_2$ solution (1 mg/mL, 0.2 mL) were illuminated by X-ray for 1 min. After 5 min, the solution was recharged. The same process was repeated for a total of 5 times. The exposure time was 5s and an "open" filter was used. All the images were processed using a Living Image software (Version 4.3.1 SP1, PerkinElmer).

XEOL imaging from beneath pork slice: *In vitro* imaging was performed by positioning LGO:Cr@mSiO$_2$ nanoparticles (0.8 mg) onto a sheet of black paper and then covered them with a 1.5-cm thick pork slice. The XEOL signals from the LGO:Cr@mSiO$_2$ nanoparticles were recorded immediately after the end of the X-ray irradiation (0.02 Gy) with the pork remained on top. After 10 min, the particles were recharged and the images were re-taken. The exposure time was 5s and an "open" filter was used. All the images were processed using a Living Image software (Version 4.3.1 SP1, PerkinElmer).

Photosensitizer loading: LGO:Cr@mSiO$_2$ nanoparticles (1 mg) were added into a 1 mL naphthalocyanine (NC) DMSO/ethanol solution (0.5 mg/mL). The mixture was stirred overnight in the dark. The dispersion was centrifuged and washed with DMSO 3 times. The

supernatant was collected after the loading process and the absorption was analyzed and compared to a pre-determined standard curve of NC. The amount of NC loaded and the loading efficiency was thus determined. The loading efficiency in wt% was computed using Equation 1:

$$\text{Photosensitizer loading (\%)} = \frac{\text{Mass of photosensitizers incorporated into particles}}{\text{Mass of particles}} \times 100 \quad (1)$$

The loading of NC was confirmed by Fourier transform infrared spectroscopy on a Nicolet iS10 FT-IR Spectrometer.

$^1O_2$ production in solutions: 1 mL NC-LGO:Cr@$mSiO_2$ solution (50 μg/mL) was added into a quartz cuvette containing 5 μM SOSG. For controls, LGO:Cr@$mSiO_2$ nanoparticles, NC, or PBS were studied. The solution was irradiated by X-ray (50 kV). The fluorescence intensities (ex/em: 504/525 nm) before and at different time points after the irradiation were measured on a Hitachi F-7000 fluorescence spectrophotometer.

*In vitro targeting imaging with H1299 cells***:** H1299 cells were grown in RPMI medium supplemented with 10% fetal bovine serum in a 37 °C incubator under 5% CO_2. Fluorescamine-labeled LGO:Cr@$mSiO_2$ and LGO:Cr@$mSiO_2$-CTX nanoparticles (0.05 mg/mL) were incubated with H1299 cells for 30 min. Fluorescamine labeling was conducted by following a published protocol.[3] Cell images were taken on an Olympus X71 fluorescence microscope.

In vitro X-PDT: H1299 lung cancer cells were grown in DMEM culture medium supplemented with 10% FBS, and 100 units/mL of penicillin. The cells were maintained in a humidified, 5% carbon dioxide (CO_2) atmosphere at 37 °C. $^1O_2$ production was estimated using SOSG assays (Life Technologies Corporation) by following the vendor's protocol.

Briefly, H1299 cells were seeded in a petri dish and grown for 24 h. The cells were prestained with 5 μM SOSG for 30 min and washed with PBS. The cells were then incubated with 50 μg/mL NC-LGO:Cr@$mSiO_2$ for 2 h before washed with PBS (3×). Cells were then irradiated by 4 Gy X-ray. After irradiation, fluorescence images were acquired on an Olympus X71 microscope using a FITC filter. Ethidium homodimer-1 assay (EthD-1 assay) was performed by following the vendor's protocol. Briefly, cells were incubated with NC-LGO:Cr@$mSiO_2$ nanoparticles (50 μg/mL) for 4 h, followed by 4 Gy X-ray irradiation. After 20 h, the cells were then incubated with 5 μM EthD-1 for 30-45 min at room temperature and washed with PBS. The images were acquired on an Olympus X71 microscope using the Tritic (red) channel.

In vivo XEOL imaging by intramuscular injection: All the animal studies were performed according to a protocol approved by the Institutional Animal Care and Use Committee (IACUC) of the University of Georgia. The *in vivo* XEOL imaging was conducted by intramuscular injection of LGO:Cr@$mSiO_2$ dispersion in phosphate-buffered saline (PBS; 1 mg mL^{-1}) into the right leg of normal nude mice at the prone position. The animals were then flipped to the supine position. The leg area was then exposed to X-ray irradiation and images in a BLI mold were immediately acquired after the irradiation (ventral view). After 10 min, the particles were recharged and the images were re-taken. The same process was repeated for a total of 5 times. The exposure time was 5s and an "open" filter was used. All the images were processed using an IVIS Lumina II in vivo imaging system (PerkinElmer Inc. Waltham, Massachusetts) with vendor-provided software (Version 4.3.1 SP1, PerkinElmer).

Establishment of orthotopic H1299 lung tumor model: The experimental techniques for establishing lung orthotopic tumors from NSCLC cells are provided in this protocol.[4] Nude mice (4–6 weeks old) were used for the animal model establishment. The aniamals were

anesthetized with isoflurane and placed in the right lateral decubitus position. H1299-luc cells (5×10^5) in matrigel were injected using a 1-mL syringe with a 28-gauge hypodermic needle. The cell inoculum was injected percutaneously into the left lateral thorax and was quickly removed after the injection of cell suspension. After tumor injection, the mouse was turned to the left lateral decubitus position. Animals were observed for 45–60 min until fully recovered. For BLI, D-luciferin was injected intraperitoneally (150 mg/kg) and BLI imaging was performed on an IVIS Lumina II in vivo imaging system (PerkinElmer Inc. Waltham, Massachusetts) to confirm tumor establishment.

In vivo XEOL targeting imaging of orthotopic H1299 lung tumor: After confirming tumor establishment (~14 days), NC-LGO:Cr@$mSiO_2$ (PEGylated) or NC-LGO:Cr@$mSiO_2$-CTX nanoparticles were intravenously injected into the H1299 tumor bearing mice (0.4 mg per animal, n=3). Before acquiring images, X-ray was applied to cover the lung area for 1 min. Images were acquired in a BLI mode immediately after the X-ray irradiation and a "Cy5.5" filter was used. All the images were processed using an IVIS Lumina II in vivo imaging system (PerkinElmer Inc. Waltham, Massachusetts) with vendor-provided software (Version 4.3.1 SP1, PerkinElmer).

In vivo X-PDT: The therapy studies were conducted in the H1299 lung tumor models, ~14 days after cell inoculation. One day before therapy, BLI was used to confirm tumor establishment on an IVIS Lumina II in vivo imaging system (PerkinElmer Inc. Waltham, Massachusetts). Based on the signals, tumor positions were marked on animal skin. The animals were randomized to receive the following treatments (n=6): 1) X-PDT: NC-LGO:Cr@$mSiO_2$-CTX (10 mg/kg) with X-ray (6 Gy), 2) X-ray only: PBS+X-ray (6 Gy), and 3) PBS only (no X-ray). For X-PDT group, NC-LGO:Cr@$mSiO_2$-CTX nanoparticles were first intravenously injected. Four hours after the injection, X-ray (6 Gy) was applied to the

tumor areas, with the rest of the body lead-shielded. BLI was performed after the therapy to assess tumor growth. After therapy, tumors and major organs from the euthanized animals were harvested, weighed, and cryosectioned. The tissue sections were then subjected to standard H&E staining to assess treatment outcomes and side effects (BBC Biochemical).

References for Experimental Section:

1. Y. J. Chuang, Z. Zhen, F. Zhang, F. Liu, J. P. Mishra, W. Tang, H. Chen, X. Huang, L. Wang, X. Chen, J. Xie and Z. Pan, *Theranostics*, 2014, 4, 1112-1122.
2. H. Chen, G. D. Wang, Y. J. Chuang, Z. Zhen, X. Chen, P. Biddinger, Z. Hao, F. Liu, B. Shen, Z. Pan and J. Xie, *Nano lett.*, 2015, 15, 2249-2256.
3. N. Dhaunta, U. Fatima and P. Guptasarma, *Anal. Biochem.*, 2011, 408, 263-268.
4. A. Onn, T. Isobe, S. Itasaka, W. Wu, M. S. O'Reilly, W. Ki Hong, I. J. Fidler and R. S. Herbst, *Clin. Cancer Res.*, 2003, 9, 5532-5539.

Supplementary Figures and Table:

Table S1. A summary of X-PDT for cancer therapy.

Publication Year	Dose rate	Transducer	size	PSs	Attachment strategy	Exp. subject	Ref.
2008	250 KV, 0.44 Gy/min	LaF_3:Tb	15 nm	MTCP	Covalent binging		1
2013	44 KV, 40 mA, 14.6 Gy	Tb_2O_3	3 nm	Porphyrin	Covalent binging		2
2015	75 kV, 20 mA	LaF_3:Tb	39 nm	Rose Bengal	Covalent binging		3
2015	75 kV, 20 mA	LaF_3:Tb	40 nm	Rose bengal	Covalent binging		4
2016	40 kV, 15 mA	$[M_6L^i_8L^a_6]^n$ com plexes	N/A	self	complex		5
2016	N/A	Au@CaPEL	130 nm	sulforhodami ne B	encapsulation		6
2007	5 Gy	ZnS:Ag, CeF_3, TiO_2, CdSe	20nm-10 μm	N/A	N/A	cell	7
2011	160 KV, 2 Gy	Y_2O_3	12 nm	psoralen	Covalent binding	cell	8
2011	120 KV, 20 mA	GdO_2S:Tb	20 μm	Photofrin II	colocation	cell	9
2014	90 KV, 5 mA, 3 Gy	LaF_3:Ce	2 μm	PPIX Phy.I.	Physical loading	cell	10
2014	120 KV, 2 Gy	ZnS:Cu,Co	4 nm	TBrRh123	Covalent binding	cell	11
2015	6 MV, 2Gy	SiC/SiOx nanowires	20 nm	H2TPACPP	Covalent binding	cell	12
2015	400 mA	GdEuC12 micelle	4.6 nm	Hyp	Physical loading	cell	13
2015	200 KV, 2 Gy	ZnO/SiO_2	98 nm	ZnO	coating	cell	14
2015	8 Gy	APTES		PPIX	coating	cell	15
2016	6 Gy, 8 KV/6 MV	CeF_3	7-11 nm	VP	Physical loading	cell	16
2014	90 KV, 5 Gy	Cu–Cy	5-30 μm	Self	No PS	Animal (it)	17
2015	220 KeV, 8 Gy	$LiYF_4$:Ce	40 nm	ZnO	coating	Animal (it)	18
2015	50 KV, 70 μA, 0.5 Gy	$SrAl_2O_4$:Eu	150 nm	MC540	Pore loading	Animal (it)	19
2016	50 KV, 70 μA, 5 Gy	$SrAl_2O_4$:Eu	150 nm	MC540	Pore loading	Animal (it)	20
2016	50 KV, 70 μA, 5 Gy	LGO:Cr	100 nm	NC	Pore loading	Animal (iv)	This study

N/A=Not available; it=introtumoral injection; iv: intravenous injection.

References for Table S1:

1. Y. F. Liu, W. Chen, S. P. Wang, A. G. Joly, *Appl. Phys. Lett.* 2008, **92**, 043901.
2. A. L. Bulin, C. Truillett, R. Chouikrat, F. Lux, C. Frochot, D. Amans, G. Ledoux, O. Tillement, P. Perriat, M. Barberi-Heyob, C. Dujardin, *J. Phys. Chem. C* 2013, **117**, 21583.
3. Y. Tang, J. Hu, A. H. Elmenoufy, X. Yang, *ACS Appl. Mater. Interfaces* 2015, **7**, 12261.
4. A. H. Elmenoufy, Y. Tang, J. Hu, H. Xu, X. Yang, *Chem. Commun.* 2015, **51**, 12247.

5. K. Kirakci, P. Kubát, K. Fejfarová, J. Martinčík, M. Nikl, K. Lang, *Inorg. Chem.* 2016, **55**, 803.
6. A. Sharmah, Z. Yao, L. Lu, T. Guo, *J. Phys. Chem. C* 2016, **120**, 3054.
7. J. Takahashi, M. Misawa, *Nanobiotechnol* 2007, **3**, 116.
8. J. P. Scaffidi, M. K. Gregas, B. Lauly, Y. Zhang, T. Vo-Dinh, *ACS Nano* 2011, **5**, 4679.
9. E. Abliz, J. E. Collins, H. Bell, D. B. Tata, *J. X-Ray. Sci. Technol.* 2011, **19**, 521.
10. X. Zou, M. Yao, L. Ma, M. Hossu, X. Han, P. Juzenas, W. Chen, *Nanomedicine* 2014, **9**, 2339.
11. L. Ma, X. J. Zou, B. Bui, W. Chen, K. H. Song, T. Solberg, *Appl. Phys. Lett.* 2014, **105**, 013702.
12. F. Rossi, E. Bedogni, F. Bigi, T. Rimoldi, L. Cristofolini, S. Pinelli, R. Alinovi, M. Negri, S. C. Dhanabalan, G. Attolini, F. Fabbri, M. Goldoni, A. Mutti, G. Benecchi, C. Ghetti, S. Iannotta, G. Salviati, *Sci. Rep.* 2015, **5**, 7606.
13. S. Kascakova, A. Giuliani, S. Lacerda, A. Pallier, P. Mercere, E. Toth, M. Refregiers, *Nano Res.* 2015, **8**, 2373.
14. R. Generalov, W. B. Kuan, W. Chen, S. Kristensen, P. Juzenas, *Colloids Surf. B* 2015, **129**, 79.
15. H. Homayoni, K. Jiang, X. Zou, M. Hossu, L. H. Rashidi, W. Chen, *Photodiagn. Photodyn. Ther.* 2015, **12**, 258.
16. S. Clement, W. Deng, E. Camilleri, B. C. Wilson, E. M. Goldys, *Sci. Rep.* 2016, **6**, 19954.
17. L. Ma, X. Zou, W. Chen, *J. Biomed. Nanotechnol.* 2014, **10**, 1501.
18. C. Zhang, K. Zhao, W. Bu, D. Ni, Y. Liu, J. Feng, J. Shi, *Angew. Chem. Int. Ed.* 2015, **54**, 1770.
19. H. Chen, G. D. Wang, Y. J. Chuang, Z. Zhen, X. Chen, P. Biddinger, Z. Hao, F. Liu, B. Shen, Z. Pan, J. Xie, *Nano Lett.* 2015, **15**, 2249.
20. G. D. Wang, H. T. Nguyen, H. Chen, P. B. Cox, L. Wang, K. Nagata, Z. Hao, A. Wang, Z. Li, J. Xie*, Theranostics* 2016, 6, 2295.

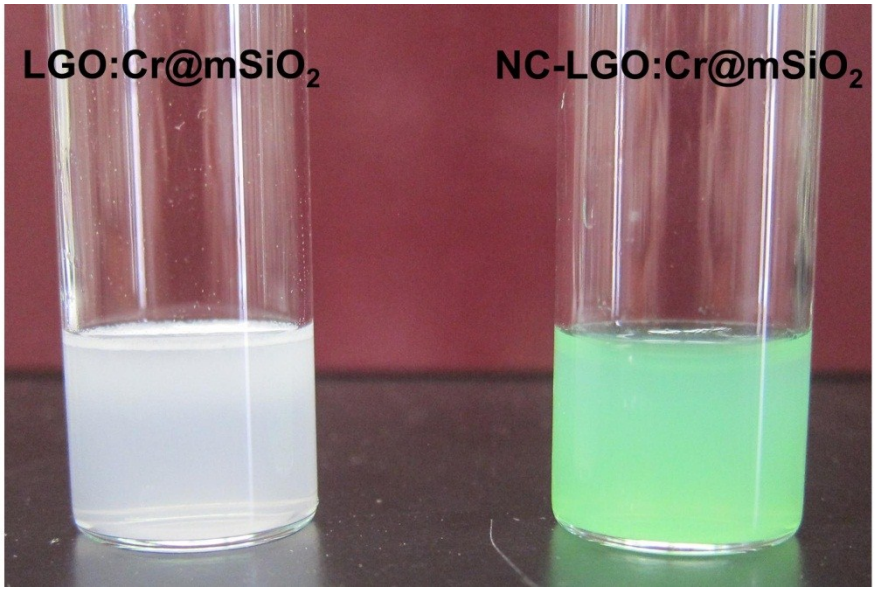

Figure S1. Stability of LGO:Cr@mSiO$_2$ and NC-LGO:Cr@mSiO$_2$ nanoparticles in aqueous solutions.

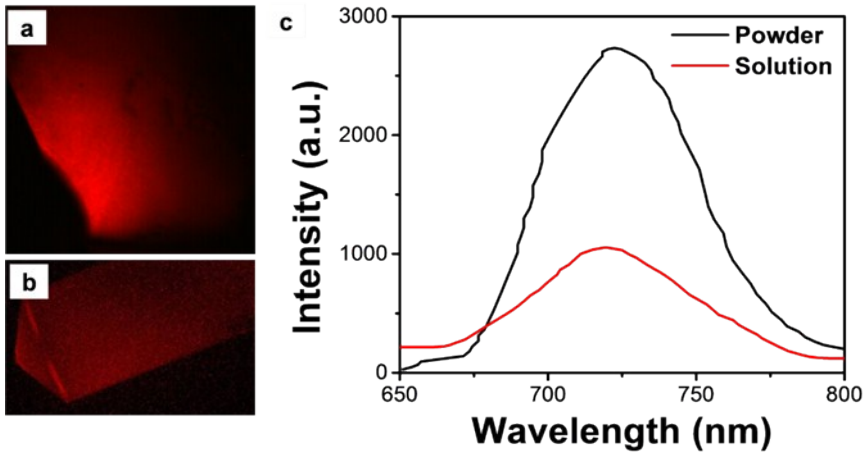

Figure S2. a) XEOL image of LGO:Cr@mSiO$_2$ nanoparticles in powders, taken on a remodeled Maestro 2 in vivo imaging system. b) XEOL image of LGO:Cr@mSiO$_2$ nanoparticle solution (1 mg/mL). c) XEOL spectra of a) and b), both of which peaked at ~720 nm.

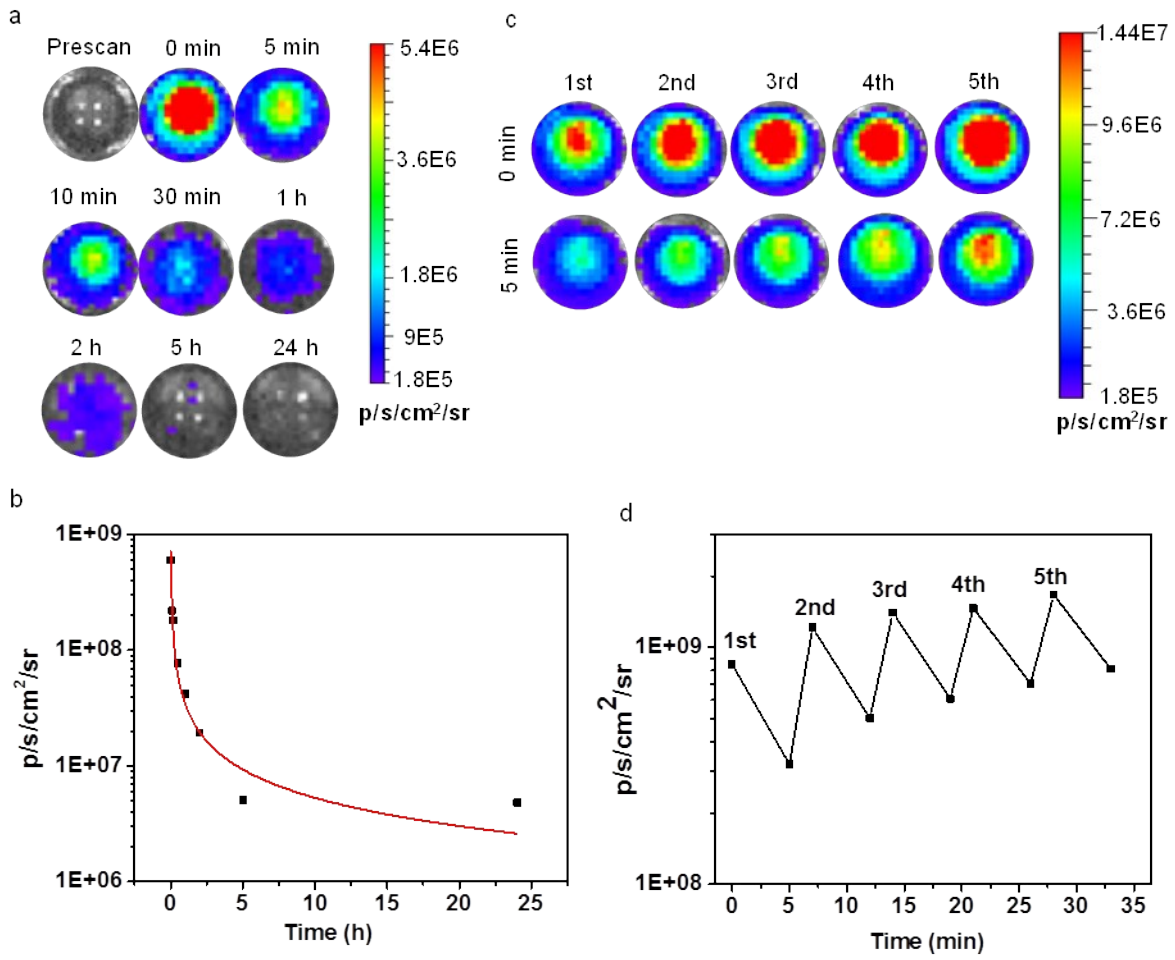

Figure S3. Phantom studies with LGO:Cr@mSiO$_2$ solutions. a) LGO:Cr@mSiO$_2$ solution (1 mg/mL, 0.2 mL) glowed in the dark after the terminus of X-ray irradiation. b) Decay curve of XEOL, based on the imaging results from a). c) LGO:Cr@mSiO$_2$ solution can re-emit after short X-ray exposure (20 cGy). The recharging can be repeated multiple times without luminescence intensity drop. d) XEOL intensity changes, based on the imaging results from c).

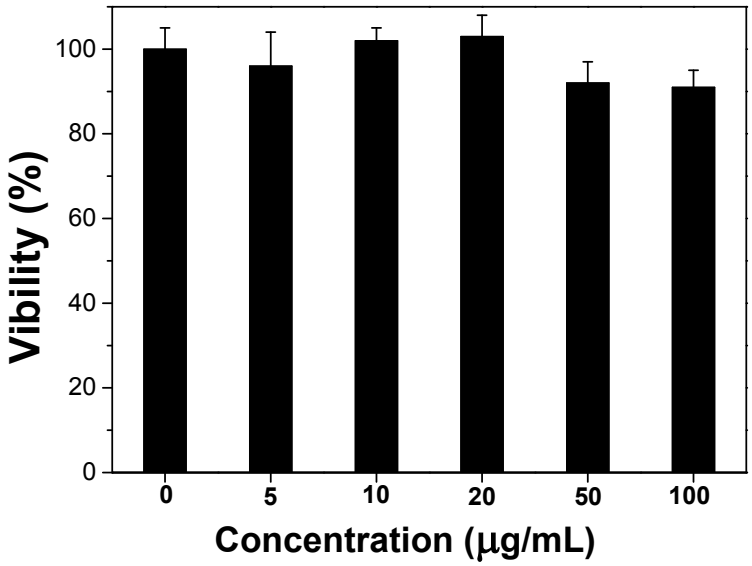

Figure S4. MTT assay results. H1299 cells were incubated with NC-LGO:Cr@mSiO$_2$ nanoparticles with different amounts in the dark.

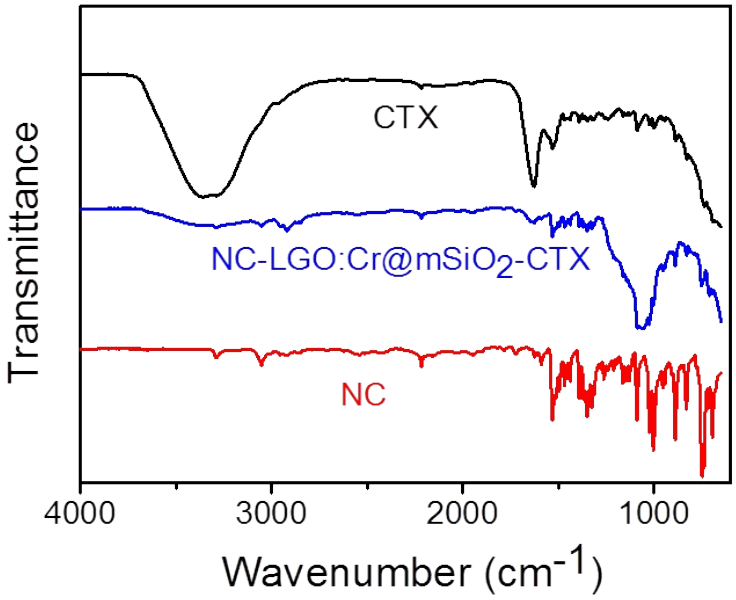

Figure S5. FT-IR of NC, CTX and NC-LGO:Cr@mSiO$_2$-CTX.

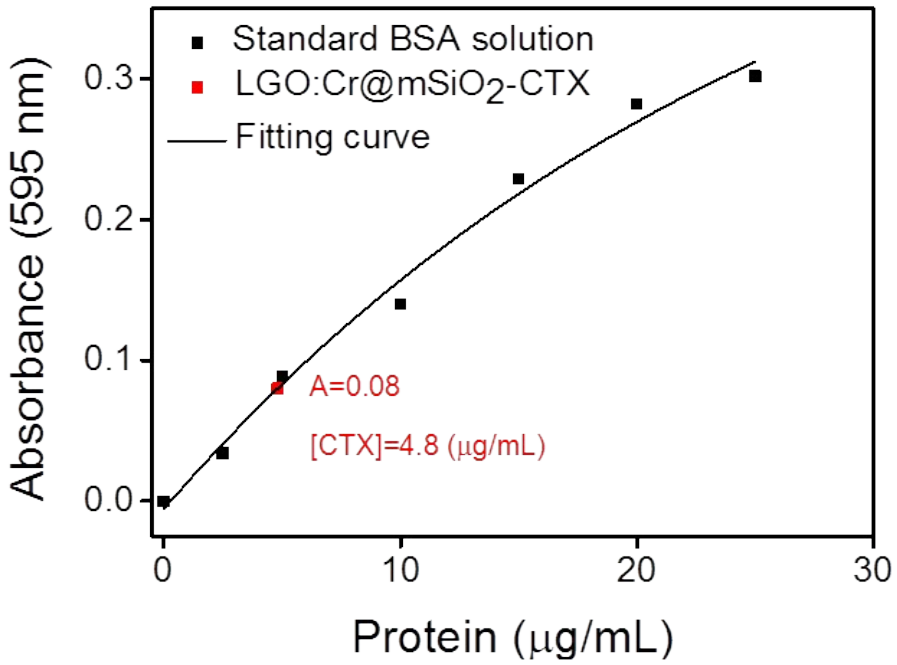

Figure S6. CTX concentration of nanoparticles was determined by Coomassie blue assay.

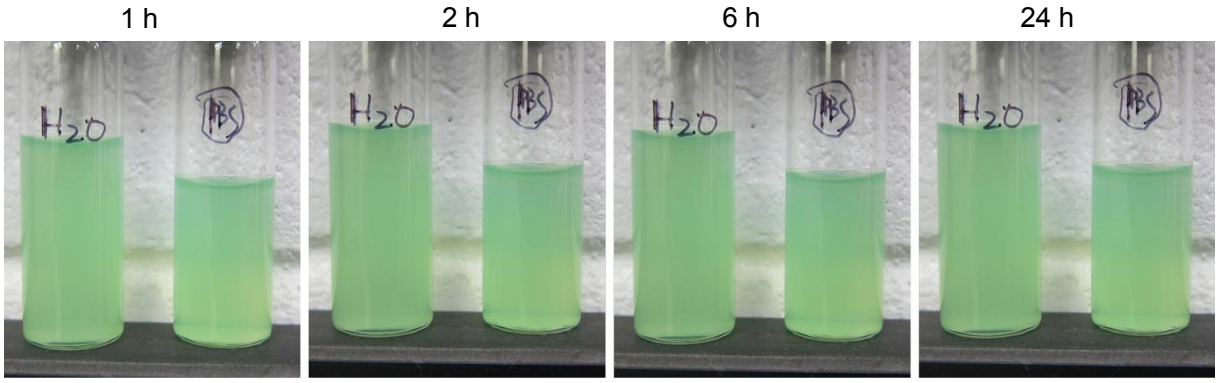

Figure S7. Stability of NC-LGO:Cr@mSiO_2-CTX in water and PBS.

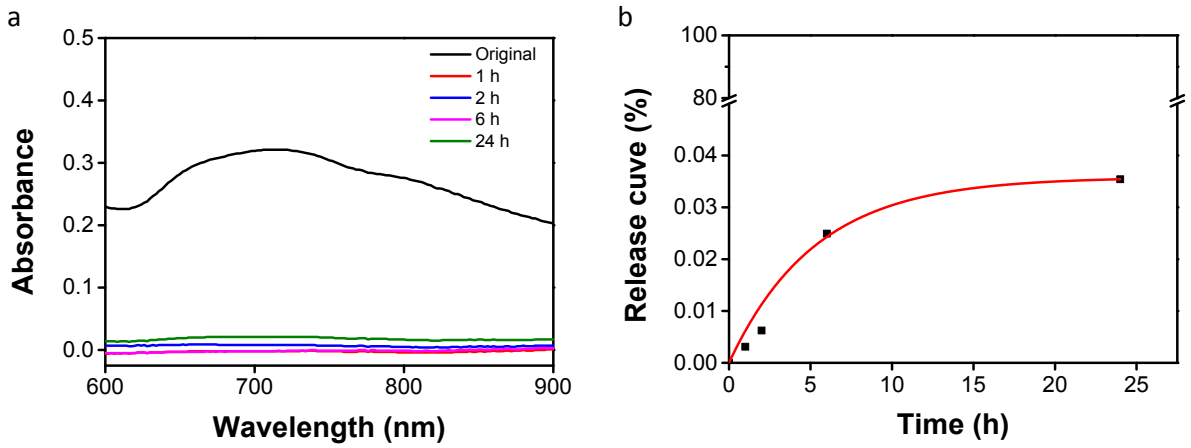

Figure S8. Release curve of NC-LGO:Cr@mSiO$_2$-CTX.

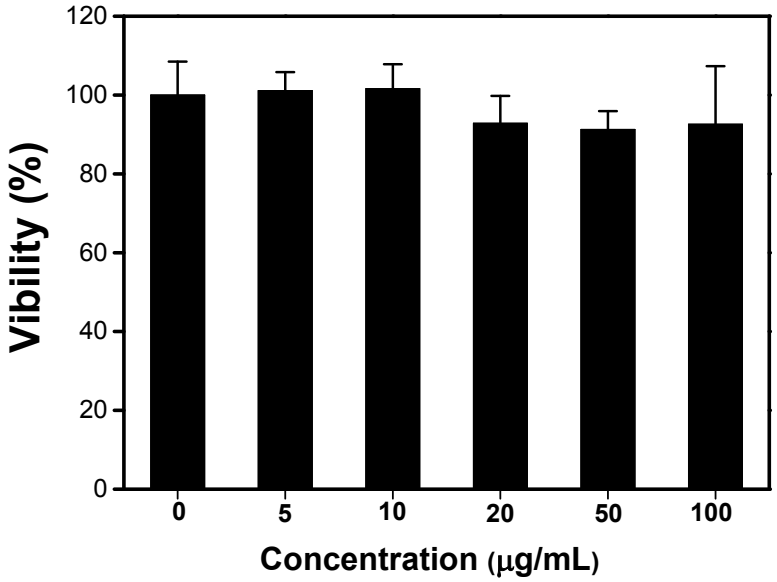

Figure S9. MTT assay results. H1299 cells were incubated with NC-LGO:Cr@mSiO$_2$-CTX nanoparticles at different concentrations in the dark.

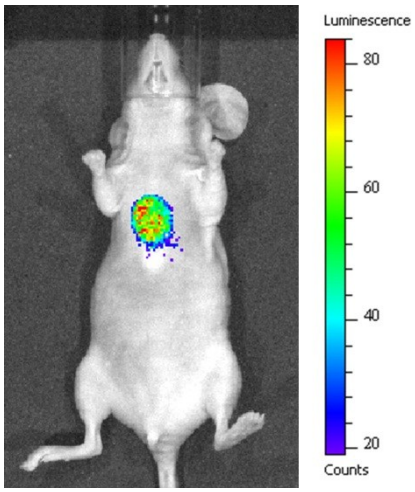

Figure S10. XEOL-guided PDT. Due to good tumor accumulation of NC-LGO:Cr@mSiO$_2$-CTX, the therapy can also be guided by XEOL from LGO:Cr after short X-ray exposure.

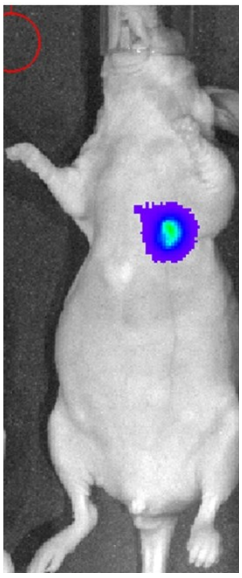

Figure S11. A representative image of mice used for therapy studies.

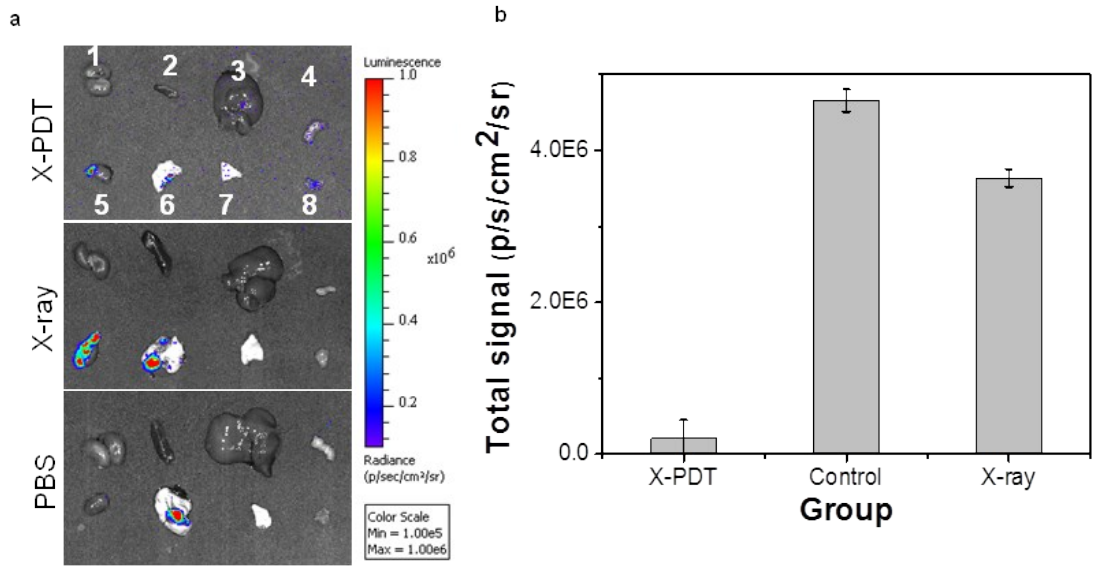

Figure S12. (a) *Ex vivo* images with dissected tissues from Figure 4. 1. kidney; 2. spleen; 3. liver; 4. Intestine; 5. heart; 6. lung; 7. Skin; 8. muscle. (b) Statistics on bioluminescent signals from a).

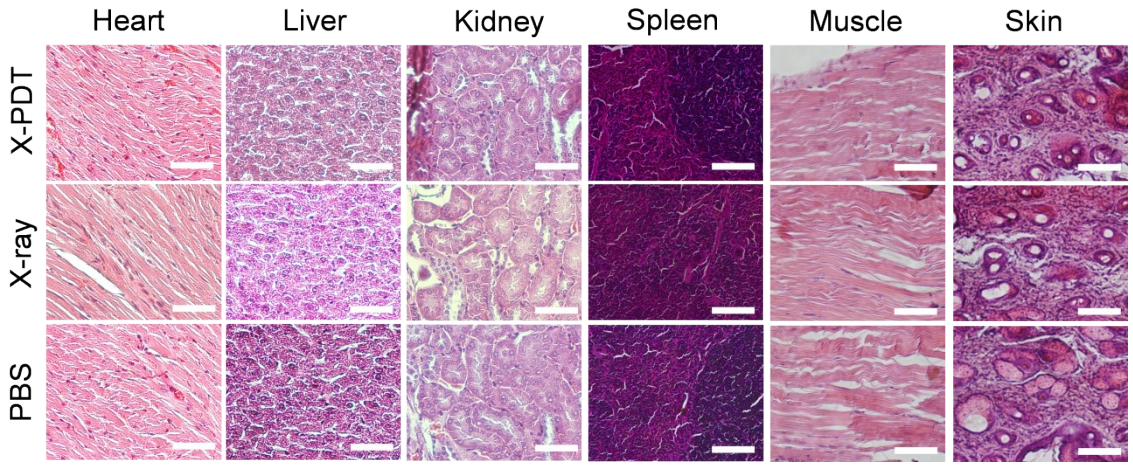

Figure S13. H&E staining of different organs after X-PDT. Aside from tumor suppression, X-PDT did cause detectable damage to normal tissues. Scale bars, 100 μm.

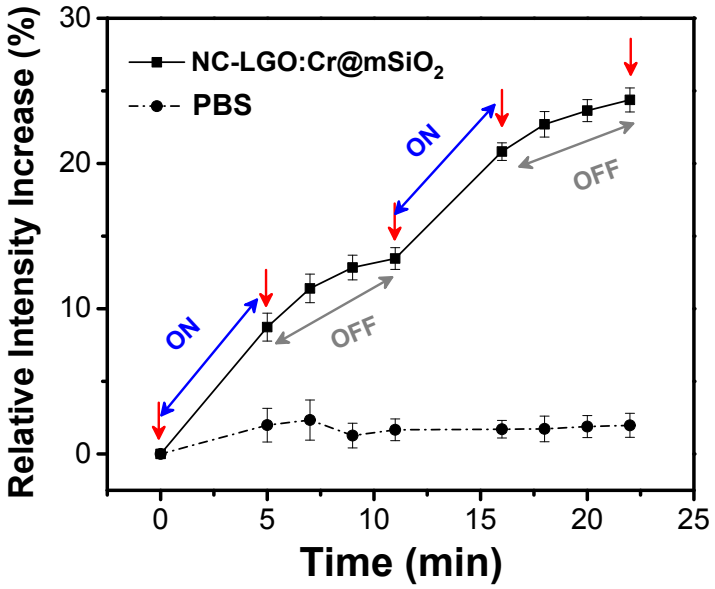

Figure S14. $^1O_2$ can be produced between the intervals of X-ray irradiation, which is attributed to the long-lasting XEOL.

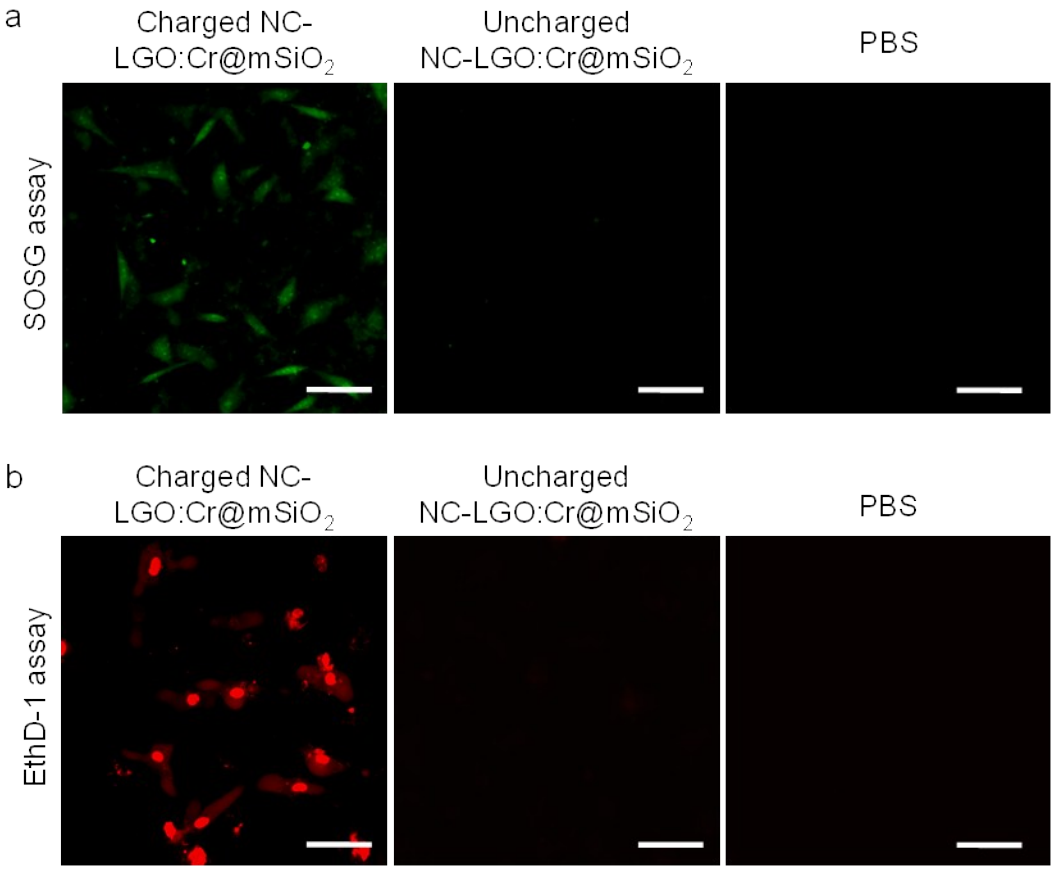

Figure S15. XEOL-mediated $^1O_2$ production and the inflicted cytotoxicity. a) $^1O_2$ production, studied with H1299 cells using SOSG as a $^1O_2$ indicator. NC-LGO:Cr@mSiO$_2$, 50 μg/mL; scale bars: 100 μm. b) Cytotoxicity study results. NC-LGO:Cr@mSiO$_2$ nanoparticles were irradiated by X-ray first (5 Gy) and then immediately added to the incubation medium of H1299 cells to a final concentration of 50 μg/mL. For controls, non-irradiated NC-LGO:Cr@mSiO$_2$ nanoparticles or PBS was added. Scale bars, 100 μm.

Table S2. Signal-to-Noise ratios based on Figure 3.

	Total Counts	Stdev	Signal-to-Noise ratios
Background	-3.39E+02	3.63E+00	1
1st-0 min	2.05E+05	1.81E+02	606
1st-5 min	7.89E+04	7.20E+01	233
1st-10 min	5.72E+04	5.66E+01	169
2nd-0 min	2.08E+05	2.56E+02	613
2nd-5 min	9.91E+04	1.13E+02	292
2nd-10 min	7.84E+04	9.19E+01	231
3rd-0 min	4.07E+05	3.87E+02	1200
3rd- 5min	1.66E+05	1.61E+02	488
3rd-10 min	1.40E+05	1.37E+02	412
4th-0 min	3.74E+05	3.83E+02	1120
4th-5 min	1.75E+05	1.78E+02	516
4th-10 min	1.49E+05	1.52E+02	440
5th-0 min	4.28E+05	4.08E+02	1260
5th-5 min	2.44E+05	2.34E+02	720
5th-10 min	1.98E+05	1.93E+02	583

Supplementary discusstion

$^1O_2$ production efficiency

The $^1O_2$ production efficiency was calculated based on a published method.[1] Briefly, the X-PDT process can be broken into three steps. Firstly, LGO:Cr nanoparticles were irradiated by X-ray to emit luminescence. Second, the XEOL activates near-by photosensitizers (NC). Lastly, $^1O_2$ is produced. From energy transformation perspective, the whole process can be regarded as a conversion from the electromagnetic energy (the ionizing radiation) to chemical energy (the $^1O_2$). The conversion efficiency (η) can be calculated from the following equation:

$$\eta = \frac{E_c}{E_{em}}$$

where E_c is the chemical energy, i.e. the energy increase when oxygen molecules are converted to singlet oxygen molecules.

The energy difference between the lowest energy of O_2 in the singlet state and the lowest energy in the triplet state is about 94.3 kJ/mol (i.e. 0.98 eV).[2,3] Therefore, E_c can be calculated from:

$$E_c = 0.98 \times N_A \times Y \text{ (J)} = 0.94 \times 10^5 \times Y \text{ (J)}$$

where N_A is the Avogadro's constant (6.02×10^{23}), 1 eV=1.6×10^{-19} J, and Y (mol) is the amount of singlet oxygen generated from the X-PDT process.

Y can be estimated from our singlet oxygen generation data (Figure 2b) using a published method.[1] When there is excess NC, the ratio between the reactants is 1:1 in the O_2-$^1O_2$-NC reaction.[1,3-6] Hence, Y is equal to the amount of the activated NC resulting from the photodynamic effect:

$$Y = n_0 \times (b_m - b_c) = W_{NC} / M_{NC} \times (b_m - b_c) = 1.4 \times 10^{-9} \times (b_m - b_c) \text{ (mol)}$$

where n_0 is the initial content of NC (2 wt% of 1 mL solution of 50 mg/L, M_{NC} = 714.77 g/mol), and (b_m-b_c) is the relative percentage change of SOSG fluorescence signals.[1] As shown in Figure 3b, the value of (b_m-b_c) is approximately equal to the difference between the control group and the NC-LGO:Cr@mSiO$_2$ group in the ordinate value at a given radiation dose. From the above two equations, E_c can be rewritten as:

$$E_c = 0.94\times10^5 \times Y = 1.3\times10^{-4}\times(b_m - b_c)\ (J)$$

Meanwhile, E_{em} is the electromagnetic energy in the form of X-ray, which is dependent on the radiation dose (D, Gy). By definition, 1 Gy is equal to an absorbed dose of 1 J/kg. Considering that 1 mL (1 g) aqueous solution was used in the experiment, E_{em} can thus be calculated as:

$$E_{em} = 1\times10^{-3}\times D\ (J)$$

Hence,

$$\eta = \frac{E_c}{E_{em}} = \frac{1.3\times10^{-4}\times(b_m - b_c)}{1\times10^{-3}\times D} = 0.13\times\frac{b_m - b_c}{D}$$

Using the above equation we computed $^1O_2$ production efficiency at different irradiation doses and the results were listed in Table S2.

Table S3. $^1O_2$ production efficiency (η) of X-PDT at different X-ray radiation doses (D) (X-ray dose rate is 0.2 Gy/min).

D/Gy	**b_m-b_c**	**η**
1	7.72%	1.00%
2	15.2%	0.99%
3	32.1%	1.39%
4	50.2%	1.63%

It can be seen that η values at different D are comparable. An average of the η values in Table 1, 1.26%, was reported in the main text.

Table S4. Size and zeta potentials of the as-synthesized particles.

	Zeta potential (mV)		Size (nm)	
	H_2O	PBS	H_2O	PBS
LGO:Cr	-17.7	-5.08	142.7	202.2
LGO:Cr@$mSiO_2$	-32.9	-5.72	157.0	242.8
LGO:Cr@$mSiO_2$-CTX	-29.6	-6.70	197.2	258.5
NC-LGO:Cr@$mSiO_2$-CTX	10.0	-1.72	259.6	296.9

References for Supplementary discusstion:

1 C. Zhang, K. Zhao, W. Bu, D. Ni, Y. Liu, J. Feng, J. Shi, *Angew. Chem. Int. Ed.* 2015, **54**, 1770.

2 C. Schweitzer, R. Schmidt, *Chem. Rev.* 2003, **103**, 1685.

3 R. Bonnett, *Chem. Soc. Rev.* 1995, **24**, 19.

4 J. F. Lovell, T. W. Liu, J. Chen, G. Zheng, *Chem. Rev.* 2010, **110**, 2839.

5 M. Shopova, D. Woehrle, V. Mantareva, S. Mueller, *J. Biomed. Opt.* 1999, **4**, 276;

6 A. Houas, H. Lachheb, M. Ksibi, E. Elaloui, C. Guillard, J. M. Herrmann, *Appl. Catal. B-Environ.* 2001, **31**, 145.